



Aalborg Universitet

AALBORG UNIVERSITY  
DENMARK

## Control of parallel-connected bidirectional AC-DC converters in stationary frame for microgrid application

Lu, Xiaonan; Guerrero, Josep M.; Teodorescu, Remus; Kerekes, Tamas; Sun, Kai; Huang, Lipei

*Published in:*

Proceedings of the 3rd IEEE Energy Conversion Congress and Exposition (ECCE 2011)

*DOI (link to publication from Publisher):*

[10.1109/ECCE.2011.6064335](https://doi.org/10.1109/ECCE.2011.6064335)

*Publication date:*

2011

*Document Version*

Early version, also known as pre-print

[Link to publication from Aalborg University](#)

*Citation for published version (APA):*

Lu, X., Guerrero, J. M., Teodorescu, R., Kerekes, T., Sun, K., & Huang, L. (2011). Control of parallel-connected bidirectional AC-DC converters in stationary frame for microgrid application. In *Proceedings of the 3rd IEEE Energy Conversion Congress and Exposition (ECCE 2011)* (pp. 4153-4160). IEEE Press.  
<https://doi.org/10.1109/ECCE.2011.6064335>

### General rights

Copyright and moral rights for the publications made accessible in the public portal are retained by the authors and/or other copyright owners and it is a condition of accessing publications that users recognise and abide by the legal requirements associated with these rights.

- Users may download and print one copy of any publication from the public portal for the purpose of private study or research.
- You may not further distribute the material or use it for any profit-making activity or commercial gain
- You may freely distribute the URL identifying the publication in the public portal -

### Take down policy

If you believe that this document breaches copyright please contact us at [vbn@aub.aau.dk](mailto:vbn@aub.aau.dk) providing details, and we will remove access to the work immediately and investigate your claim.

# Control of Parallel-Connected Bidirectional AC-DC Converters in Stationary Frame for Microgrid Application

Xiaonan Lu<sup>1</sup>, Josep Guerrero<sup>2,3</sup>, Remus Teodorescu<sup>2</sup>, Tamas Kerekes<sup>2</sup>, Kai Sun<sup>1</sup> and Lipei Huang<sup>1</sup>

1. State Key Lab of Power Systems, Department of Electrical Engineering, Tsinghua University, Beijing, China

2. Department of Energy Technology, Aalborg University, Aalborg, Denmark

3. Dept. Enginyeria de Sistemes Automàtica i Informàtica Industrial Universitat Politècnica de Catalunya

**Abstract—** With the penetration of renewable energy in modern power system, microgrid has become a popular application worldwide. In this paper, parallel-connected bidirectional converters for AC and DC hybrid microgrid application are proposed as an efficient interface. To reach the goal of bidirectional power conversion, both rectifier and inverter modes are analyzed. In order to achieve high performance operation, hierarchical control system is accomplished. The control system is designed in stationary frame, with harmonic compensation in parallel and no coupled terms between axes. In this control system, current/voltage controllers and droop controllers are reached in the first level. Controllers to restore the deviation caused by droop are achieved in the second level. To improve the performance in grid-connected operation, tertiary control can be involved. Theoretical analyses of main power circuit and control diagram are validated by simulation and experiment.

## I. INTRODUCTION

With the progress of industry application, problems caused by the gradually decreasing of fossil fuel and environment pollution are shown clearly nowadays. As a result, renewable energy sources are playing more important role in the modern energy system [1, 2]. With the rapid development of renewable energy technology, great attention is paid to ‘Microgrid’ worldwide. Microgrid is a kind of power grid area which is a combination of different kinds of power units which are usually based on renewable energy sources [3-6]. A hybrid microgrid can be made up of distributed renewable source, AC and DC common buses, interface circuit and local load. In the application of microgrid, power electronics converter is usually adopted as an interface circuit to guarantee the reliable and efficient connection of both AC and DC sides [7].

In this paper, bidirectional parallel-connected three-phase converters are employed. The control goal is to achieve a bidirectional ‘bridge’ in AC and DC hybrid microgrid. Also, it can be employed to connect energy storage units, in order to accomplish charging and discharging process. At the present stage, only standalone rectifier and inverter operation modes are analyzed. The transient results of switching between the two modes will be shown in the probable future work.

To achieve high performance operation of bidirectional parallel converter system, hierarchical control in stationary

frame is adopted. Hierarchical control structure is composed of different control levels. AC/DC voltage and current control and power sharing between the parallel converters are achieved. At the same time, reduction of deviation caused by droop controllers is also reached.

Concretely, in this paper, hierarchical control strategies are derived for both standalone rectifier and inverter operation modes. Models of the main power circuit in time domain and control diagram in frequency domain are shown respectively. Simulation based on Matlab/Simulink is done and test on a 2×2.2kW prototype is performed to validate the feasibility of the parallel converter system.

## II. MODELING AND CONTROL OF PARALLEL CONVERTER SYSTEM

The proposed control diagram of the converter is shown in Fig.1. The same for the second converter, only the control structure for Converter 1 is shown in detail. It can be seen that the control system is achieved in both rectifier and inverter modes. The hierarchical structure can be shown as follow. In the first control level, Proportional-Resonant (PR) controller for AC voltage or current and Proportional-Integrator (PI) controller for DC voltage are employed. Also, droop controllers for DC current sharing and AC active and reactive power sharing are accomplished. In the second level, DC voltage controller in rectifier operation and AC frequency/amplitude controllers in inverter operation are achieved to restore the deviation caused by droop. Finally, when considering the connection to a stiff AC or DC source, tertiary control can be involved. Since the control system is accomplished in stationary frame, it is easy to employ harmonic compensation (HC) in parallel and no cross-coupled terms between axes exist.

### A. Rectifier Operation

First, rectifier operation is analyzed as follow. From Fig.1, the state equations of the system in a-b-c frame can be obtained. With the transformation from a-b-c to  $\alpha$ - $\beta$ , the state equations in stationary frame can be reached. For isolated transformer is adopted, zero-sequence path is cut off. So, zero-axis is not considered here. As a result, the main power circuit model of

the parallel rectifier system in  $\alpha$ - $\beta$  frame can be shown in Fig.2. It can be seen clearly that different from the model in d-q frame,

there are no coupled terms between the state variables between different axes within one converter.

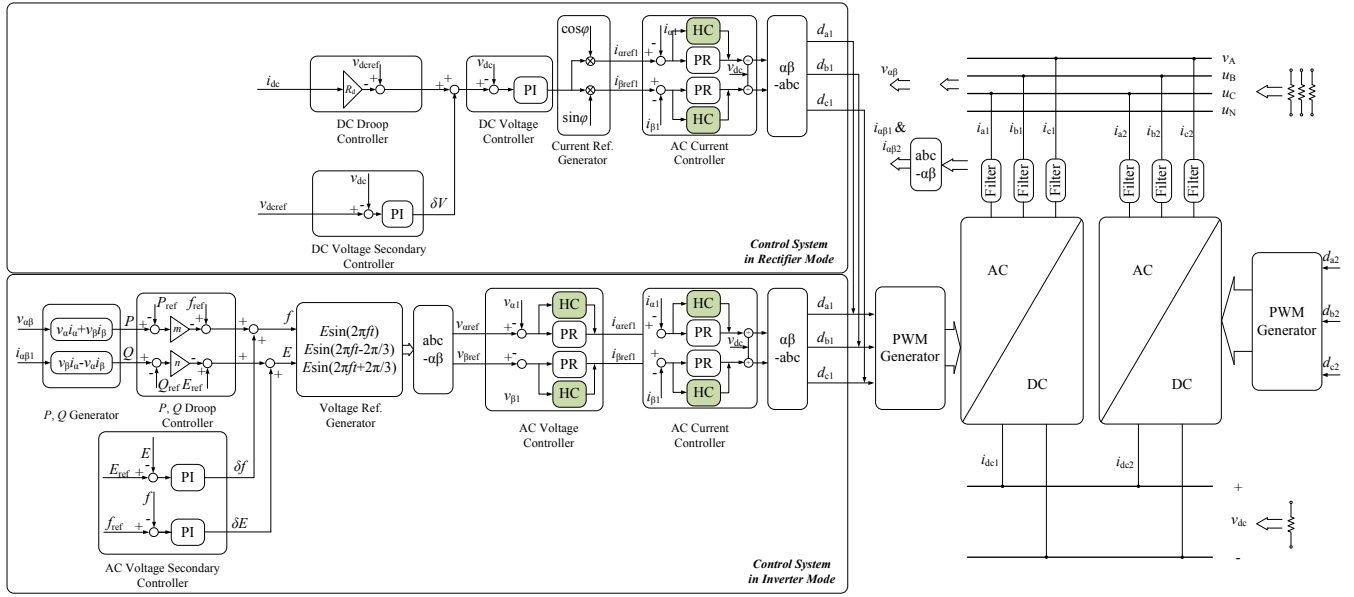


Fig.1 Control diagram of the whole system

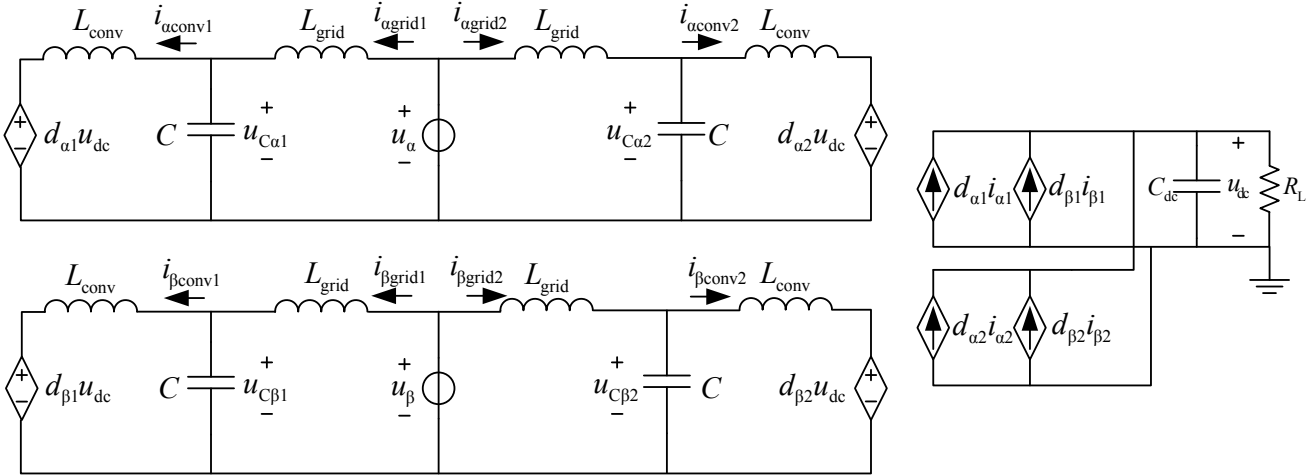


Fig.2 Main power circuit model for parallel rectifiers

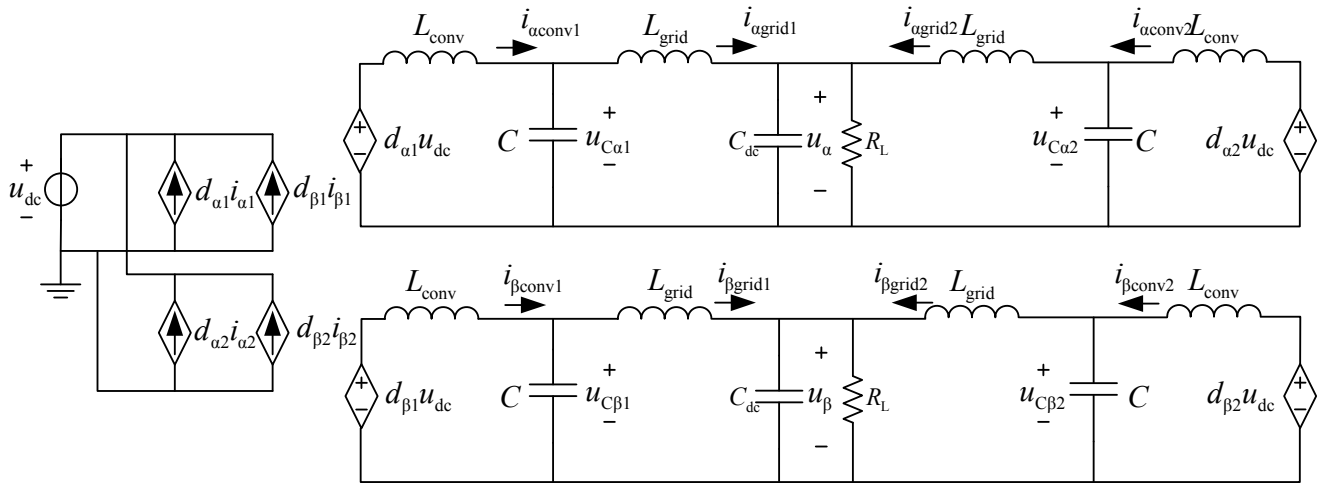


Fig.3 Main power circuit model for parallel inverters

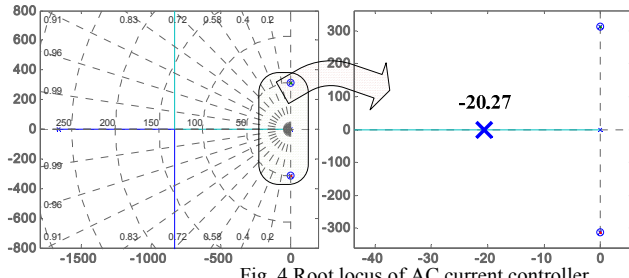


Fig. 4 Root locus of AC current controller (Normal-left, partial enlarged-right)

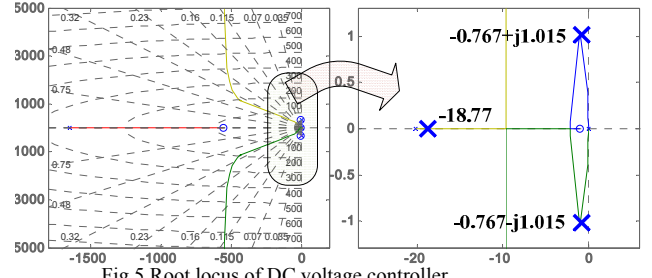


Fig. 5 Root locus of DC voltage controller (Normal-left, partial enlarged-right)

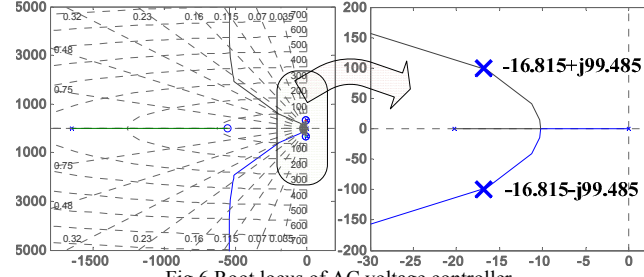


Fig. 6 Root locus of AC voltage controller (Normal-left, partial enlarged-right)

With the above model in time domain, design of hierarchical control system in frequency domain can be reached. In the PR AC current controller, to reach a bandwidth of 1050Hz,  $K_p$  is set to 16 and  $K_r$  is set to 3000. At the same time, in the PI DC voltage controller, to reach a bandwidth of 200Hz,  $K_p$  is set to 1.3 and  $K_i$  is set to 6. Root locus diagram of the two controllers are shown in Fig.4 and 5. Here, damping resistor is involved to maintain the stability of the system and only dominant poles are shown. It can be tested that the parallel rectifier system is stable with the above parameters. After designing the AC current and DC voltage loops, droop controller in the first control level should be employed. In parallel rectifier system, droop effect is shown by means of DC current sharing. The virtual resistor  $R_d$  is selected to guarantee a maximum of 3% DC voltage deviation of its normal value. Suppose that in a parallel rectifier system, the load resistor in the DC side is 200Ω. Then  $R_d$  should be less than 12Ω.

To restore the deviation of the DC voltage caused by droop, secondary controller is designed. PI controller with low bandwidth communication is required here. The parameters of the controller is selected as  $K_p=0.003$  and  $K_i=13$ .

For standalone operation of the parallel system is analyzed in the paper, tertiary controller designed for grid-connected mode is not involved.

### B. Inverter Operation

Similar to those in rectifier situation, the state equations in  $\alpha$ - $\beta$  frame can be achieved and the main power circuit model of the parallel inverter system derived from the state equations is shown in Fig.3. For space limitation of the paper, detailed derivation is not shown here. Also, it can be seen clearly that, different from the model in d-q frame, there are no coupled terms between the state variables in different axes within one converter.

As same as that in the rectifier mode, hierarchical control system is designed in frequency domain with the above model

in time domain. In the first control level, PR AC current controller is adopted. And also, for the voltage here is in the AC side, PR voltage controller is employed. In the PR current controller, to reach a bandwidth of 1050Hz,  $K_p$  is set to 16 and  $K_r$  is set to 3000. And in the PR voltage controller, to reach a bandwidth of 200Hz and,  $K_p$  is set to 0.35 and  $K_r$  is set to 500. AC current controller is exactly the same as that in rectifier mode, so its root locus diagram is not described repeatedly. Root locus of AC voltage controller is shown in Fig.6. Only dominant poles are shown here. It can be tested that the parallel inverter system is stable with the above parameters. Also in the first control level, droop controller is designed. In inverter mode, droop controller is employed to reach active and reactive power sharing. In order to guarantee a maximum of 3% of frequency and amplitude deviation, the droop coefficient ' $m$ ' and ' $n$ ' are achieved as 0.00008 and 0.18 respectively. For decoupling of active and reactive power, the output impedance of each inverter should be inductive or resistive. The inductive impedance leads to the relationships of  $P$ - $f$  and  $Q$ - $E$ . On the other hand, the resistive impedance leads to the relationships of  $P$ - $E$  and  $Q$ - $f$ . Here, inductive virtual impedance of 4mH 1Ω is adopted, to maintain the inductive AC output impedance.

To restore the amplitude and frequency of AC voltage, PI secondary controller with low bandwidth communication is designed. The parameters of the controllers for amplitude is selected as  $K_{pe}=0.00012$  and  $K_{ie}=0.13$  and the those of the controller for frequency is selected as  $K_{pf}=0.0005$  and  $K_{if}=0.6$ .

Also, for standalone operation of the parallel system is analyzed in the paper, tertiary controller designed for grid-connected mode is not involved.

## III. SIMULATION VALIDATION

### A. Rectifier Operation

To test the performance of parallel converter system, simulation based on Matlab/Simulink is accomplished. The

parameters of the system are shown in Table I. The parameters adopted in both simulation and experiment are the same.

In parallel rectifier operation, the steady state waveforms of DC voltage and AC current are shown in Fig.7 and 8. It can be seen that in steady state, DC voltage is well regulated to the reference value and the AC current is in sinusoidal shape as desired.

The effect of droop control is shown in Fig.9. With droop control, the difference between DC output currents is lowered down from 1.46A to 0.19A.

The effect of secondary control is shown in Fig.10. With secondary control, the deviation of DC voltage is well restored.

It should be notice that, for clear expression, results with and without droop control are shown together in Fig.9.

### B. Inverter Operation

The steady state waveforms of AC voltage and current are shown in Fig.11 and 12. It can be seen that both AC voltage and current are in sinusoidal shape as desired.

The effect of droop control is shown in Fig.13 and 14. To active power, with droop control, the difference between active power outputs is lowered down from 347W to 12W and the difference between reactive power outputs is reduced from 285Var to 44Var.

The effect of secondary control is shown in Fig.15 and 16. With secondary control, the deviation of frequency and amplitude are well restored.

Also, for clear expression, different results with or without droop control are shown together in Fig.13 and 14.

In order to reach high performance operation of parallel converter system, HC is involved. To show its effect, harmonic analysis of AC current for Converter 1 in both rectifier and inverter modes is accomplished, as shown in Table II.

TABLE I  
SIMULATION AND EXPERIMENT PARAMETERS

|                           |     |  |     |                             |                  |
|---------------------------|-----|--|-----|-----------------------------|------------------|
| DC Ref. Voltage (V)       | 700 | Filter Inductance (Grid & Inverter Sides) (mH) | 1.8 | Switching Frequency (kHz)   | 8                |
| AC Ref. Voltage (rms) (V) | 230 | Filter Capacitor ( $\mu$ F)                    | 9   | Converter Power Rating (kW) | 2 $\times$ 2.2kW |

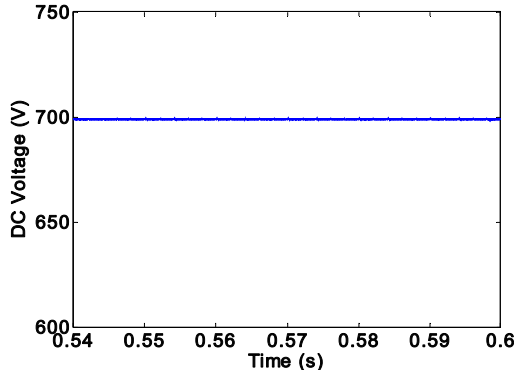


Fig.7 Steady state of DC voltage (Rectifier)

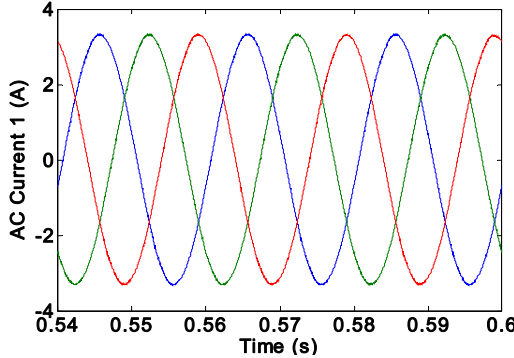


Fig.8 Steady state of AC current (Rectifier)

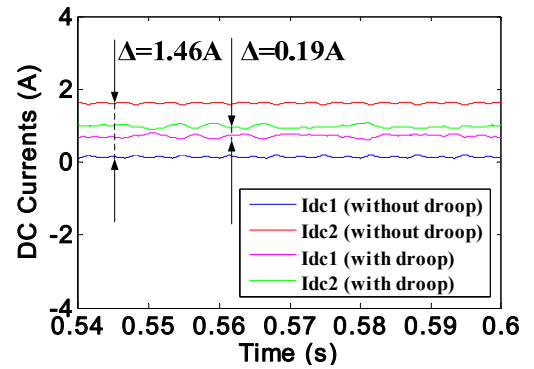


Fig.9 DC current sharing by droop control (Rectifier)

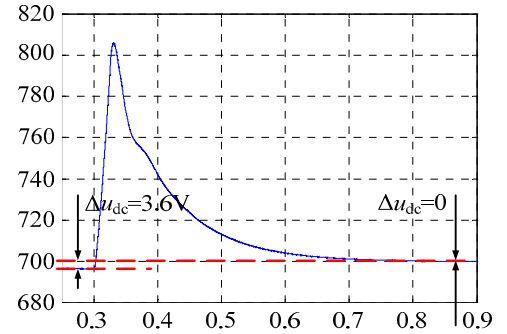


Fig.10 DC voltage restoration of secondary control (Rectifier)

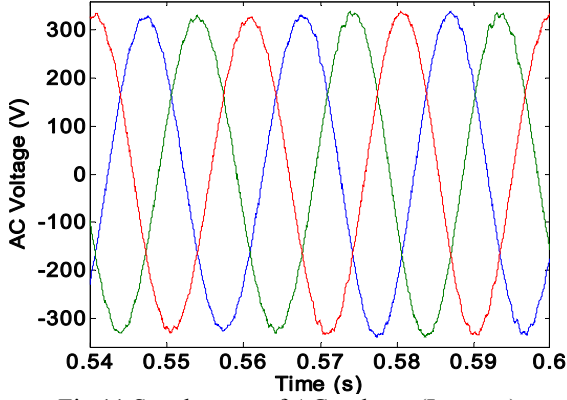


Fig.11 Steady state of AC voltage (Inverter)

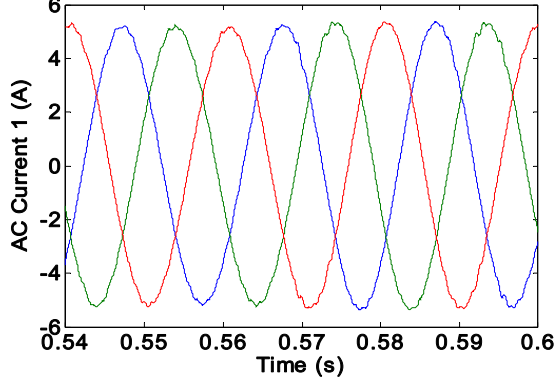


Fig.12 Steady state of AC current (Inverter)

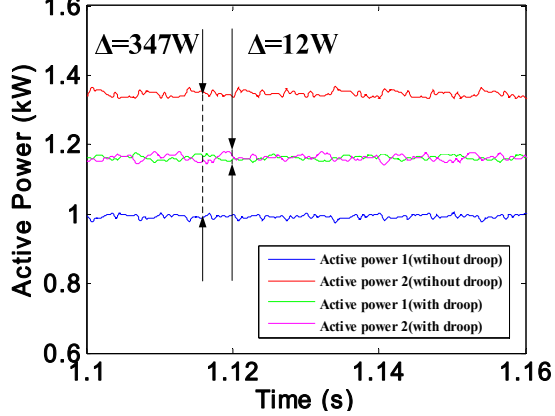


Fig.13 AC active power sharing by droop control (Inverter)

TABLE II

HARMONIC ANALYSIS RESULTS OF AC Current (SIMULATION)

|            | Rectifier Operation   |                       |           | Inverter Operation    |                       |           |
|------------|-----------------------|-----------------------|-----------|-----------------------|-----------------------|-----------|
|            | 5 <sup>th</sup><br>/% | 7 <sup>th</sup><br>/% | THD<br>/% | 5 <sup>th</sup><br>/% | 7 <sup>th</sup><br>/% | THD<br>/% |
| Without HC | 2.33                  | 3.23                  | 8.13      | 1.33                  | 6.44                  | 7.23      |
| With HC    | 0.69                  | 0.11                  | 1.07      | 0.19                  | 0.02                  | 1.32      |

#### IV. EXPERIMENT VALIDATION

##### A. Rectifier Operation

A 2×2.2kW prototype is implemented to verify the performance of the parallel converter system [5]. The parameters of the experiment setup are the same as that in simulation. The structure of the system is shown in Fig.17.

In parallel rectifier operation, steady state waveforms of DC voltage and AC current are shown respectively in Fig.18 and 19.

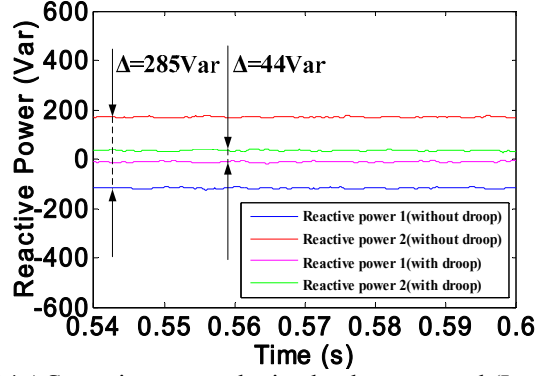


Fig.14 AC reactive power sharing by droop control (Inverter)

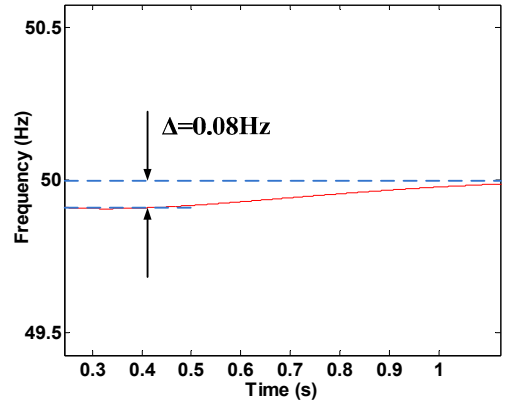


Fig.15 Frequency restoration of secondary control (Inverter)

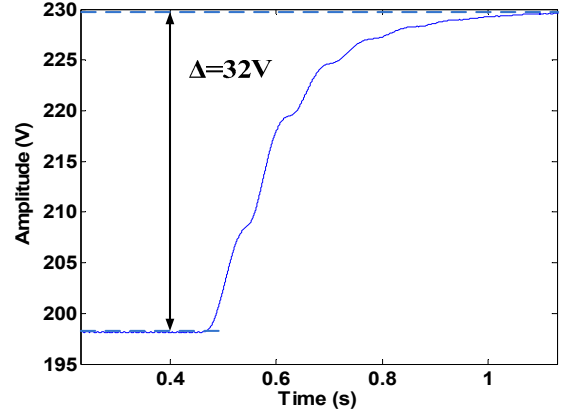


Fig.16 Amplitude restoration of secondary control (Inverter)  
It can be seen that both DC voltage and AC current waveforms meet the requirements.

With droop control, the DC current values are shown in Table III. Here, resistance load of 400Ω is adopted in the DC side. At the same time, the influence of DC voltage caused by droop control is shown in Fig.20.

With secondary control, the deviation of DC voltage can be restored, as shown in Fig.21.

TABLE III

DC CURRENT VALUES WITH DROOP CONTROL

| DC Load | $i_{dc1}/A$ | $i_{dc2}/A$ | $\Delta i_{dc}/A$ |
|---------|-------------|-------------|-------------------|
| 400Ω    | 0.82        | 0.77        | 0.05              |

##### B. Inverter Operation

In parallel inverter operation, steady state waveforms of AC voltage and AC current are shown respectively in Fig.22 and 23.

It can be seen that both AC voltage and current waveforms meet the requirement.

With droop control, the active and reactive power in the AC side are shown in Table IV. Here, both inductive and resistive load are tested. At the same time, the influence of AC voltage caused by droop control is shown in Fig.24.

With secondary control, the deviation of AC voltage can be restored, as shown in Fig.25 and 26. Considering the influence in practical system, it will spend longer time to restore the frequency and amplitude. Also, ‘Sampling & Hold’ module is employed to verify the low bandwidth communication.

In order to test the effect of HC, 5<sup>th</sup> and 7<sup>th</sup> harmonics and the THD of AC current is monitored. As same as that in simulation,

AC current for Converter 1 is selected as an example.

Experiment harmonic analysis results for both rectifier and inverter operations are shown in Table V.

TABLE IV  
AC ACTIVE AND REACTIVE POWER VALUES WITH DROOP CONTROL

| AC Load                 | $P_1/W$ | $P_2/W$ | $\Delta P/W$ | $Q_1/Var$ | $Q_2/Var$ | $\Delta Q/Var$ |
|-------------------------|---------|---------|--------------|-----------|-----------|----------------|
| 230 $\Omega$            | 337.7   | 338.1   | -0.4         | 6.04      | -3.81     | 9.85           |
| 115 $\Omega$ ,<br>600mH | 63.1    | 76.5    | -13.4        | 105.34    | 106.79    | -1.45          |

TABLE V  
HARMONIC ANALYSIS RESULTS OF AC Current (EXPERIMENT)

|            | Rectifier Operation |                    |       | Inverter Operation |                    |       |
|------------|---------------------|--------------------|-------|--------------------|--------------------|-------|
|            | 5 <sup>th</sup> /%  | 7 <sup>th</sup> /% | THD/% | 5 <sup>th</sup> /% | 7 <sup>th</sup> /% | THD/% |
| Without HC | 3.00                | 3.90               | 8.00  | 0.90               | 6.90               | 8.70  |
| With HC    | 0.40                | 0.90               | 4.50  | 0.76               | 0.90               | 5.00  |

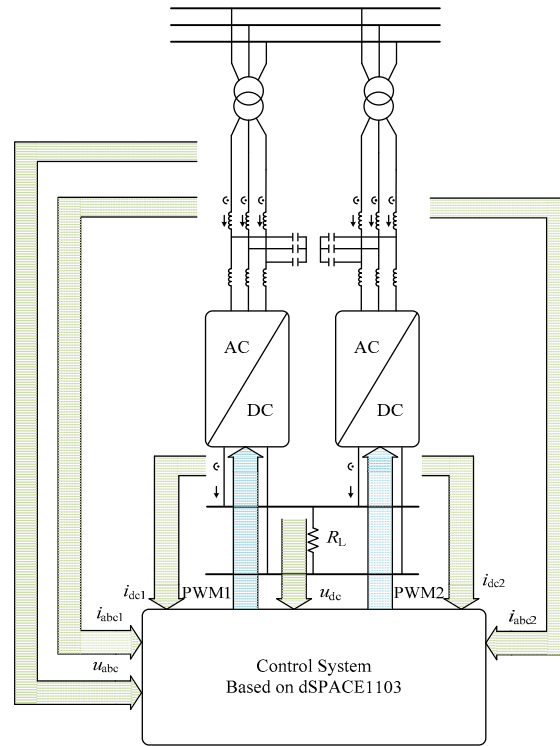


Fig.17 Experiment system structure

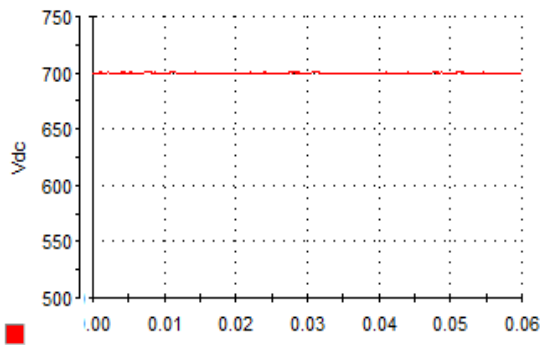


Fig.18 Steady state of DC voltage (Rectifier)

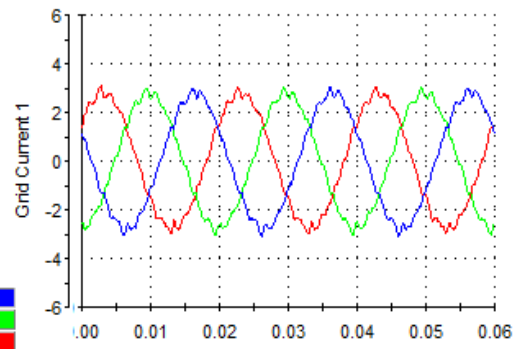


Fig.19 Steady state of AC current (Rectifier)



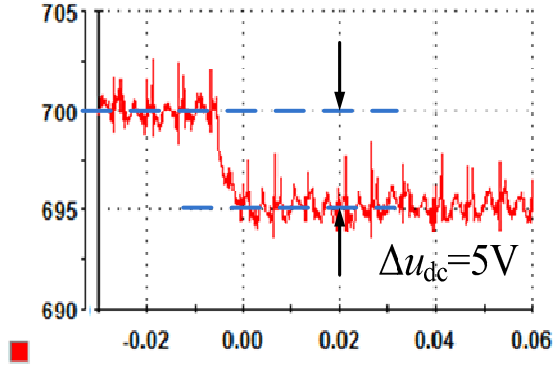


Fig.20 Influence of DC voltage caused by droop control

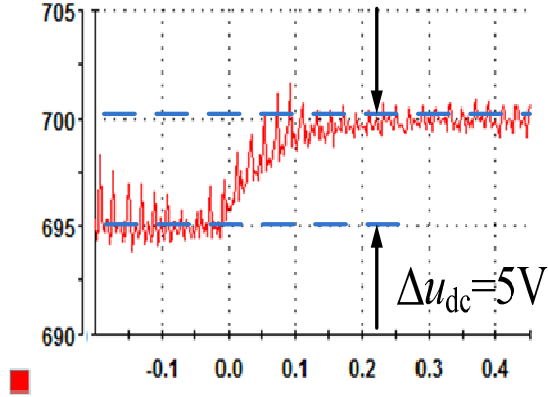


Fig.21 DC voltage restoration of secondary control (Rectifier)

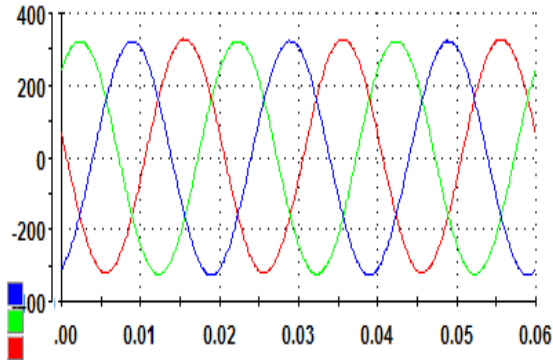


Fig.22 Steady state of AC voltage (Inverter)

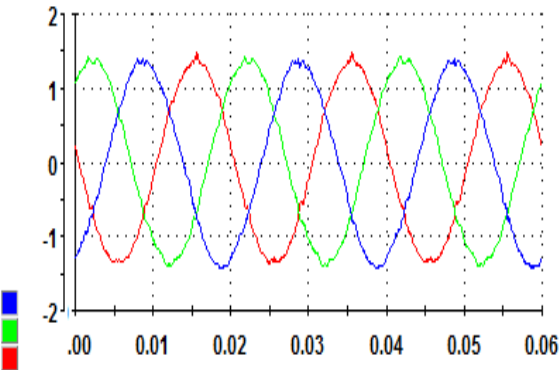


Fig.23 Steady state of AC current (Inverter)

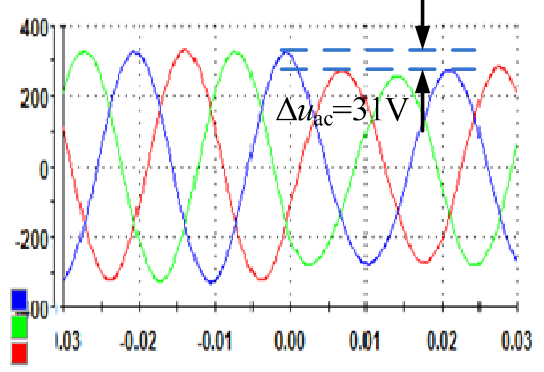


Fig.24 Influence of AC voltage caused by droop control

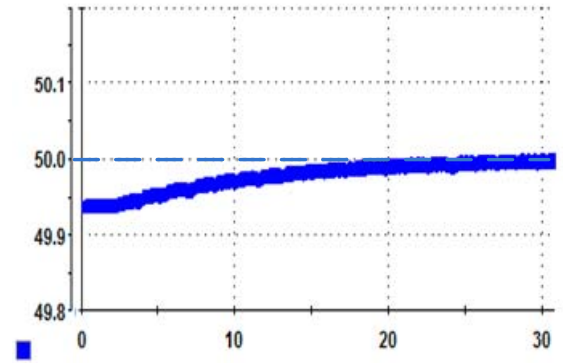


Fig.25 Frequency restoration of secondary control (Inverter)

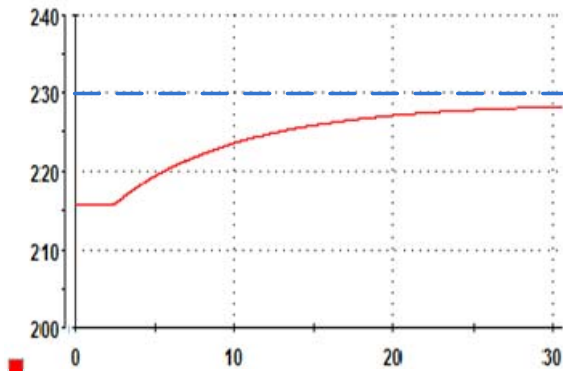


Fig.26 Amplitude restoration of secondary control (Inverter)

## V. SUMMARY

In this paper, parallel-connected bidirectional three-phase converters are employed as an interface in AC and DC hybrid microgrid. Model of main power circuit in time domain and hierarchical control system in frequency domain are shown. In the first level of the control system, AC voltage and current controllers (PR), DC voltage controller (PI) and droop controller are achieved. In the second level, DC voltage controller (PI), AC frequency and amplitude controllers (PI) are employed to restore the deviation caused by droop. The control system is achieved in stationary-frame, in order to easily involve parallel HC and avoid coupled terms between different axes. Simulation and experiment results validate the *reliable* operation of the system. To reach the goal of bidirectional operation, all the theoretical analyses, simulation



and experiment results are accomplished in both rectifier and inverter operation modes.

#### ACKNOWLEDGEMENT

This work is supported by grants from the Power Electronics Science and Education Development Program of Delta Environmental & Educational Foundation (DREG2010007) and also by China Scholarship Council for high level postgraduate.

#### REFERENCES

- [1] F. Blaabjerg, R. Teodorescu, M. Liserre and A.V. Timbus. "Overview of control and grid synchronization for distributed power generation systems," *IEEE Transactions on Industrial Electronics*, Vol.53, No.5, 2006:1398-1409.
- [2] E. Figueres, G. Garcera, etc. "Sensitivity study of the dynamics of three-phase photovoltaic inverters with an LCL grid filter," *IEEE Transactions on Industrial Electronics*, Vol. 56, No. 3, 2009:706-717.
- [3] J. M. Guerrero, J. C. Vasquez, J. Matas, etc. "Control strategy for flexible microgrid based on parallel line-interactive UPS system," *IEEE Transactions on Industrial Electronics*, Vol.56, No.3, 2009:726-736.
- [4] I.Y. Chung, W.X. Liu, etc. "Control methods of inverter-interfaced distributed generators in a microgrid system," *IEEE Transactions on Industry Applications*, Vol.46, No.3, 2010:1078-1088.
- [5] J.C. Vasquez, J.M. Guerrero, A. Luna, etc. "Adaptive droop control applied to voltage-source inverters operating in grid-connected and islanded modes," *IEEE Transactions on Industrial Electronics*, Vol.56, No.10, 2009:4088-4096.
- [6] Y.W. Li, D.M. Vilathgamuwa, P.C. Loh. "A grid-interfacing power quality compensator for three-phase three-wire microgrid applications," *IEEE Transactions on Power Electronics*, Vol.21, No.4, 2006:1021-1031.
- [7] F. Blaabjerg, Z. Chen, S.B. Kjaer. "Power electronics as efficient interface in dispersed power generation systems," *IEEE Transactions on Power Electronics*, Vol.19, No.5, 2004:1184-1194.